

Unlock your experimental potential  
with power and agility  
**BD FACSymphony™ A5 SE Cell Analyzer**  
Discover the difference >



## Diversity of Antigen-Specific Responses Induced In Vivo with CTLA-4 Blockade in Prostate Cancer Patients

This information is current as of February 26, 2022.

Serena S. Kwek, Vinh Dao, Ritu Roy, Yafei Hou, David Alajajian, Jeffrey P. Simko, Eric J. Small and Lawrence Fong

*J Immunol* 2012; 189:3759-3766; Prepublished online 5 September 2012;  
doi: 10.4049/jimmunol.1201529  
<http://www.jimmunol.org/content/189/7/3759>

**Supplementary Material** <http://www.jimmunol.org/content/suppl/2012/09/05/jimmunol.1201529.DC1>

**References** This article **cites 28 articles**, 17 of which you can access for free at:  
<http://www.jimmunol.org/content/189/7/3759.full#ref-list-1>

**Why *The JI*? Submit online.**

- **Rapid Reviews! 30 days\*** from submission to initial decision
- **No Triage!** Every submission reviewed by practicing scientists
- **Fast Publication!** 4 weeks from acceptance to publication

*\*average*

**Subscription** Information about subscribing to *The Journal of Immunology* is online at:  
<http://jimmunol.org/subscription>

**Permissions** Submit copyright permission requests at:  
<http://www.aai.org/About/Publications/JI/copyright.html>

**Email Alerts** Receive free email-alerts when new articles cite this article. Sign up at:  
<http://jimmunol.org/alerts>



# Diversity of Antigen-Specific Responses Induced In Vivo with CTLA-4 Blockade in Prostate Cancer Patients

Serena S. Kwek,\* Vinh Dao,\* Ritu Roy,<sup>†</sup> Yafei Hou,\* David Alajajian,\* Jeffrey P. Simko,<sup>‡</sup> Eric J. Small,\* and Lawrence Fong\*

CTLA-4 is a surface receptor on activated T cells that delivers an inhibitory signal, serving as an immune checkpoint. Treatment with anti-CTLA-4 Abs can induce clinical responses to different malignancies, but the nature of the induced Ag-specific recognition is largely unknown. Using microarrays spotted with >8000 human proteins, we assessed the diversity of Ab responses modulated by treatment with CTLA-4 blockade and GM-CSF. We find that advanced prostate cancer patients who clinically respond to treatment also develop enhanced Ab responses to a higher number of Ags than nonresponders. These induced Ab responses targeted Ags to which preexisting Abs are more likely to be present in the clinical responders compared with nonresponders. The majority of Ab responses are patient-specific, but immune responses against Ags shared among clinical responders are also detected. One of these shared Ags is PAK6, which is expressed in prostate cancer and to which CD4<sup>+</sup> T cell responses were also induced. Moreover, immunization with PAK6 can be both immunogenic and protective in mouse tumor models. These results demonstrate that immune checkpoint blockade modulates Ag-specific responses to both individualized and shared Ags, some of which can mediate anti-tumor responses. *The Journal of Immunology*, 2012, 189: 3759–3766.

Cancer immunotherapy relies on the induction of effector T cells to mediate tumor regression. Activation of these T cells requires recognition of specific Ags in concert with costimulatory signals from the CD28 receptor on T cells. CD28, which is constitutively expressed on T cells, binds to the CD80 and CD86 molecules present on the cell surface of APCs and delivers signals required by naive T cells to become activated and proliferate (1). Once activated, these T cells transiently upregulate the CTLA-4 receptor on their cell surface, which interacts with the same ligands as CD28, but serves as an immune checkpoint, inhibiting cell cycle progression and IL-2 production (2). Thus, CTLA-4 signaling provides negative feedback to activated T cells, thereby dampening an immune response. Blocking of CTLA-4 with anti-CTLA-4 Abs enhances effector T cell responses and can induce T cell-mediated rejection of certain tumors in mouse

models (3). Anti-CTLA-4 Ab treatment possesses anti-tumor activity in cancer patients with different tumor types (4) and is a U.S. Food and Drug Administration-approved drug shown to improve survival of patients with metastatic melanoma. Clinical trials in many other cancers are under way including two phase III trials in men with metastatic castration-resistant prostate cancer (CRPC) (<http://www.ClinicalTrials.gov>; identifiers NCT00861614 and NCT01057810).

CTLA-4 blockade has been shown to induce T cell and humoral immunity to Ags in mice that are vaccinated with defined antigenic peptides (5) or whole-cell tumor vaccines (6). In cancer patients, CTLA-4 blockade can induce Abs to the cancer-testis Ag, NY-ESO-1 (7), but these responses are not tightly associated with clinical responses for prostate cancer (8) and therefore may not mediate the anti-tumor effects seen. CTLA-4 blockade can also induce Abs to MHC class I chain-related protein A in melanoma patients vaccinated with irradiated, autologous tumor cells transduced to express GM-CSF (9). GM-CSF is a cytokine that regulates the survival, proliferation, differentiation, and function of granulocytes, macrophages, and dendritic cells (10, 11) and that has been shown to synergize with CTLA-4 in preclinical and clinical trials (12). CTLA-4 blockade can also induce significant clinical responses without a concomitant vaccine. This treatment presumably potentiates an adaptive immune response to the endogenous tumor Ags, but the immunologic targets that mediate anti-tumor activity are largely unknown.

We performed a phase I trial where a combination of anti-CTLA-4 Ab (ipilimumab; Bristol-Myers Squibb) and GM-CSF (sargramostim; Sanofi) was administered to patients with metastatic CRPC who had not received any prior chemotherapy or immunotherapy. We found that this treatment induced clinical responses at or above a dose threshold of 3 mg/kg anti-CTLA-4 (8). At dose levels of 3 mg/kg and 10 mg/kg anti-CTLA-4, 5 of 11 evaluable patients had a prostate-specific Ag (PSA) response to the treatment, defined by a serum PSA level decline of 50% or greater from the highest PSA level. On the basis of this criterion, we could separate the study subjects into clinical responders

\*Division of Hematology/Oncology, Department of Pathology, University of California, San Francisco, San Francisco, CA 94143; <sup>†</sup>Helen Diller Family Comprehensive Cancer Center, Biostatistics and Computational Biology Core, University of California, San Francisco, San Francisco, CA 94143; and <sup>‡</sup>Department of Pathology, University of California, San Francisco, San Francisco, CA 94115

Received for publication June 5, 2012. Accepted for publication July 30, 2012.

This work was supported by the National Cancer Institute (R01-CA136753 to V.D. and L.F. and R01-CA163012 to L.F.), the Peter Michael Foundation (to S.S.K.), the University of California San Francisco Prostate Cancer Specialized Program of Research Excellence (to J.P.S., E.J.S., and L.F.), and the Prostate Cancer Foundation (to Y.H. and E.J.S.). Equipment support was provided by the University of California San Francisco Clinical and Translational Science Institute (National Institutes of Health National Center for Research Resources UL1 RR024131).

The protein array data presented in this article have been submitted to the National Center for Biotechnology Information Gene Expression Omnibus (<http://www.ncbi.nlm.nih.gov/geo/>) under accession number GSE39688.

Address correspondence and reprint requests to Dr. Lawrence Fong, University of California, San Francisco, 513 Parnassus Avenue, Box 0511, San Francisco, CA 94143. E-mail address: lawrence.fong@ucsf.edu

The online version of this article contains supplemental material.

Abbreviations used in this article: CAMK, calcium/calmodulin-dependent protein kinase; CRPC, castration-resistant prostate cancer; EM, estimation-maximization; PSA, prostate-specific Ag; UCSF, University of California, San Francisco.

Copyright © 2012 by The American Association of Immunologists, Inc. 0022-1767/12/\$16.00

(patients 19, 20, 24, 33, 36) and nonresponders (patients 21, 22, 23, 28, 34, 35; Fig. 1A). As these patients did not receive cancer vaccines as part of their treatment, this clinical study provides an opportunity to determine the endogenous Ags against which immune responses are induced with immune checkpoint blockade-based immunotherapy. High-density human protein arrays were used to profile the Ag-specific immune responses in these prostate cancer patients receiving anti-CTLA-4 Ab and GM-CSF. We find that clinical responders develop Ag-specific immune responses distinct from clinical nonresponders. We also demonstrate that an identified shared autoantigen can also serve as a novel tumor-associated Ag.

## Materials and Methods

### Clinical trial

A phase I/II trial combined escalating doses of anti-CTLA-4 Ab (ipilimumab; Bristol-Myers Squibb) with a fixed dose of GM-CSF (sargramostim; Sanofi) was performed to assess for safety, feasibility, and immunogenicity in patients with CRPC (NCT00064129) (8). Patients received up to four doses of anti-CTLA-4 Abs at the specified doses. These doses were given in 4-wk cycles with GM-CSF administered daily on the first 14 d of these cycles. Cycles of GM-CSF treatment could continue until disease progression or toxicity. The characteristics of patients are summarized in Supplemental Table I. Sera and cryopreserved PBMCs from study subjects who received ipilimumab at the 3 mg/kg ( $n = 6$ ) and 10 mg/kg ( $n = 6$ ) doses were used in this study. A sixth patient in the 10 mg/kg cohort discontinued the study after 2 mo due to disease progression, so posttreatment samples were not available in that patient. Informed consent was obtained for investigations on humans.

### IgG profiling with high-density protein microarrays

Sera from pretreatment and from posttreatment (month 6) were diluted 1:500 in probing buffer and used to blot protein arrays (Invitrogen) according to the manufacturer's instructions. Abs bound to the spotted proteins were detected by using anti-human IgG conjugated to Alexa Fluor 647 (Invitrogen), and fluorescence was acquired with a GenePix fluorescence microarray axon scanner (Molecular Devices, Sunnyvale, CA).

### Statistical analysis

**Preprocessing.** The data were transformed into  $\log_2$  intensity values. Spots whose  $\log_2$  intensity values were below array-specific low-intensity cutoffs were excluded from analyses by setting them as missing. The array-specific low-intensity thresholds were determined as the 75th percentile of the  $\log_2$  intensity values of the negative control spots. Duplicate spots were averaged. The data were then normalized using quantile normalization to ensure that the intensities had the same empirical distribution across arrays. Lastly, each array was median-centered. All protein array data have been deposited in the National Center for Biotechnology Information Gene Expression Omnibus database under accession number GSE39688 (<http://www.ncbi.nlm.nih.gov/geo/query/acc.cgi?acc=GSE39688>) and is MIAME compliant.

**Unsupervised clustering of protein arrays.** Cluster and Treeview software (13) were used for unsupervised clustering of the data with Pearson correlation and complete linkage.

For each array, an Ag was identified as being detected if its value was above the median. To determine the number of up- and downmodulated Abs, the difference in  $\log_2$  intensity values of pretreatment and posttreatment samples were taken for each patient to identify Ags that are detected differentially due to treatment. Number of Abs with at least 2- or 4-fold difference {difference in  $\log_2$  intensity values =  $\pm 1$  or  $\pm 2$ } between pretreatment and posttreatment samples was compared between responders and nonresponders by performing two-sided Wilcoxon rank sum test and using the 5% level of significance.

To determine the number of upmodulated Abs that have preexisting levels or not in the pretreatment serum, normal mixture modeling with estimation-maximization (EM) as implemented in the mclust package in R (14) was applied to the raw intensities for each pretreatment and posttreatment array to identify the boundary between non-preexisting and preexisting (Supplemental Fig. 1A, 1B). Normal mixture modeling assumes that the data consist of two or more subsets that have different distributions (normal distributions with different parameters) and tries to identify the distributions and hence the Abs that belong to those distributions by using the EM algorithm. The raw intensities were subjected to preprocessing as before, and

all  $\log_2$  values were centered to the boundary, and values below the boundary were set to zero. The number of Abs upmodulated by 2- or 4-fold in the posttreatment serum that were preexisting in the pretreatment serum was compared with the number of similarly upmodulated Abs that were non-preexisting in the pretreatment serum for each patient. Fisher exact tests were performed for each patient, and the  $p$  values were adjusted for multiple comparisons by Bonferroni method. An adjusted  $p$  value cutoff of 0.05 was used to determine significance. Odds ratios were estimated from conditional maximum likelihood estimates. Multiplicative Poisson regression model with the number of Abs upmodulated as the dependent variable and clinical response status and pretreatment preexisting or not status as dependent variables were fitted to see if there was any interaction between clinical response and pretreatment Abs.

All statistical analyses were performed by using R/Bioconductor software (14, 15) unless otherwise mentioned.

### Intracellular cytokine staining

PBMCs were incubated with media alone (IMDM, 5% human sera, 2 mM L-glutamine, 100 U/ml penicillin and 0.1 mg/ml streptomycin), or with 10  $\mu$ g/ml baculoviral purified human PAK6 or CAMK2N1 protein, or 50 ng/ml PMA and 500 ng/ml ionomycin. Anti-human CD28 Ab (BD Bioscience) and anti-human CD49d Ab (BD Bioscience) were added at a final concentration of 1  $\mu$ g/ml for 48 h. GolgiStop buffer (BD Bioscience) was added at a final concentration of 1  $\mu$ g/ml for the last 6 h. The cells were stained with 1  $\mu$ g/ml of all Abs unless otherwise noted. Cells were first stained with allophycocyanin-conjugated anti-human CD3 Ab (BioLegend), Pacific blue-conjugated anti-human CD4 (BioLegend), PE-Cy7-conjugated anti-human IL-4 (eBioscience), and allophycocyanin-conjugated anti-human CD20 (BD Bioscience) for 1 h at room temperature and fixed and permeabilized with standard methods (BioLegend Fox Fix/Perm buffer). Cells were then stained intracellularly with Alexa 700-conjugated anti-human IFN- $\gamma$  (BioLegend) or PE-conjugated anti-human IL-17A Ab (eBioscience) and assessed by flow cytometry. Results were analyzed with FlowJo software (Tree Star).

### Western blotting and immunohistochemistry

Cell lines were lysed in lysis buffer (20 mM HEPES pH 7.4, 150 mM NaCl, 1.5 mM  $MgCl_2$ , 1 mM EGTA, 10% Triton X-100, and protease inhibitors), and 30  $\mu$ g of total protein was loaded per lane of an SDS-PAGE. Primary Abs used for Western blotting: goat anti-human PAK6 at 1:400 dilutions (1  $\mu$ g/ $\mu$ l, AF4265; R&D Systems); mouse anti-human  $\beta$ -actin at 1:10,000 dilutions (2  $\mu$ g/ $\mu$ l, A1978; Sigma). Secondary Abs: HRP-conjugated anti-goat IgG (1  $\mu$ g/ $\mu$ l; Upstate) or HRP-conjugated anti-mouse IgG (1  $\mu$ g/ $\mu$ l; Upstate) at 1:5000 dilutions.

Paraffin-embedded prostate tumors were baked, deparaffinized, and rehydrated in the following order with xylene, 100% EtOH, 95% EtOH, 70% EtOH, and distilled water. The slides were then pressure cooked in 10 mM citrate buffer pH 6, washed in distilled water and in PBS with 0.05% Tween 20, and incubated in 3%  $H_2O_2$  in PBS for 15 min. Slides were first blocked with normal goat serum (S-1000; Vector Labs) diluted 1:10 and incubated with the primary staining Abs [rabbit anti-human PAK6, 1  $\mu$ g/ $\mu$ l (Novus Biologicals), or normal rabbit IgG control, 1  $\mu$ g/ $\mu$ l (Dako)] at 1:200 dilutions overnight at 4°C. The slides were next incubated with biotinylated goat anti-rabbit (1.5  $\mu$ g/ $\mu$ l, BA-1000; Vector Labs) at 1:200 dilutions, ABC-HRP (PK-6100 Vectastain ABC kit; Vector Labs) at 1:100 dilutions, and with 3,3'-diaminobenzidine (D5905; Sigma) for 5 min at room temperature. Images were obtained with an Olympus microscope (BX41) with attachment (U-DO3) and camera (Micropublisher 5.0). The objective lens used was  $\times 20/0.4$  Plan, and the resulting magnification was  $\times 200$ . The acquisition software used was QCapture.

### T cell proliferation assay

C57BL/6 and FVB mice were immunized twice with CFA plus PBS or CFA plus PAK6 protein (100 mg/mouse) (three mice in each immunized group) 14 d apart. After an additional 14 d, the mice were sacrificed, and sera and cells from the inguinal draining lymph nodes were obtained. Lymphocytes derived from draining lymph nodes were cocultured in triplicate at  $3 \times 10^5$  cells/well with media alone (RPMI 1640, 10% FBS, 2 mM L-glutamine, 25 mM HEPES, 0.1 mM nonessential amino acids, 100 U/ml penicillin and 0.1 mg/ml streptomycin) (negative control), or with 0.5  $\mu$ g/ml, 2.5  $\mu$ g/ml, or 5  $\mu$ g/ml baculoviral purified PAK6 or CAMK2N1 proteins, or with 5 ng/ml *Staphylococcus aureus* enterotoxin A (Sigma) (positive control) for 4 d at 37°C. Cells were pulsed with 1 mCi/well [ $^3H$ ]thymidine (16), harvested after 24 h, and DNA was collected onto a membrane filter. Radioactive counts per minute were determined with a MicroBeta counter (PerkinElmer). Assays were performed in triplicate wells. Animal care was

performed in accordance with institutional guidelines. Immunized mice were monitored for clinical signs of autoimmunity including manifestation rash and weight loss. Normal tissues including prostate, seminal vesicles, testis, liver, and brain were assessed for inflammatory infiltrates by H&E staining.

### ELISPOT assay

PBMCs ( $2 \times 10^5$ ) from spleen cells of immunized mice as described for the proliferation assay were plated in media per well in triplicate in MultiScreen filter plates (Millipore) coated with 1  $\mu$ g/ml capture anti-human IFN- $\gamma$  Abs in PBS and previously blocked with media. Cells were incubated at 37°C for 24 h. Plates were washed with PBS, incubated overnight with 1  $\mu$ g/ml of detection anti-human IFN- $\gamma$  biotin-conjugated Abs in PBS, and detected with streptavidin-HRP and AEC substrate (BD Biosciences). Assays were performed in triplicate wells.

### Tumor challenge

C57BL/6 and FVB mice (five mice in each group) were immunized with CFA plus PBS and CFA plus PAK6 (100 mg) twice, 14 d apart. Then,  $2 \times 10^5$  Tramp cells for C57BL/6 or  $2 \times 10^5$  Myc-Cap cells for FVB mice were injected s.c. into their flank 14 d after the last immunization. Tumor growth was monitored three times a week. Per institutional protocol, mice were euthanized when the tumor size reached 2 cm in maximal dimension.

## Results

### Modulation of autoantibody responses with CTLA-4 blockade-based treatment

Subjects were classified as clinical responders or nonresponders by whether the individual experienced a 50% or greater decline in his serum PSA levels (Supplemental Table II). Clinical responders had stable bone scans on treatment, and one of the clinical responders had regression of liver metastasis (8). The median time to PSA level progression in clinical responders was 416 d (range, 336–2000-plus

d) compared with 103 d (range, 73–176 d) in the nonresponders. Pretreatment and posttreatment sera of the treated study subjects were used to screen for IgG Abs that bind to high-density protein arrays containing 8274 unique recombinant human proteins that were spotted in duplicate on glass slides. These protein arrays have been validated for detecting Abs to known and potentially novel tumor-associated Ags (17). We observed that anti-CTLA-4 and GM-CSF treatment modulate Ab responses to a variety of different autoantigens. Ab responses to specific Ags are both up- and downmodulated after treatment. The intensity values were quantile normalized,  $\log_2$  transformed, and centered with respect to the global median. Scatterplots of the fluorescence intensities were analyzed comparing pretreatment to posttreatment levels for each patient (Fig. 1B, 1C). Upmodulated and downmodulated Ab responses between pretreatment and posttreatment Ab intensities were compared between responders and nonresponders. Clinical responders have a higher frequency of 4-fold upmodulated Abs with treatment compared with the nonresponders (two-sided Wilcoxon rank sum test,  $p < 0.05$ ), whereas there is no significant difference in downmodulated Abs between the two groups (Fig. 1D).

### Detection of patient-specific and shared autoantibody responses induced by treatment

Unsupervised hierarchical clustering of the patients and Ags were carried out with Pearson correlation as the distance metric and complete linkage as the agglomeration method (Fig. 2A). Pretreatment and posttreatment sera from individual patients cluster together, indicating that modulated immune responses are of a lesser magnitude than differences between patients. Notably, the Ab profiles of the clinical responders 19, 20, and 36 cluster to-

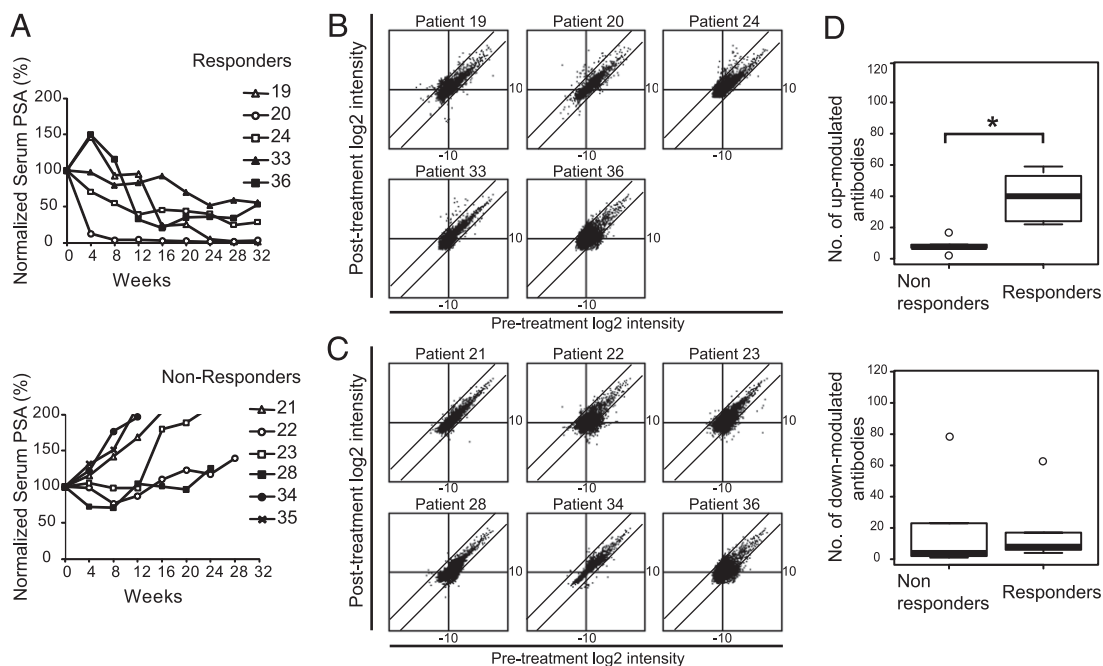


**FIGURE 1.** Modulation of Ag-specific IgG responses with CTLA-4 blockade. (A) Serum PSA levels of prostate cancer patients treated with CTLA-4 blockade normalized to the baseline level are plotted over weeks after the initiation of treatment. Subjects received ipilimumab at either 3 mg/kg (filled symbols) or 10 mg/kg (open symbols). PBMCs and sera from these patients were used for subsequent experiments. (B) Scatterplot analysis of median-centered,  $\log_2$ -transformed and normalized fluorescence intensities are plotted for pretreatment ( $x$ -axis) and posttreatment ( $y$ -axis) sera from clinical responders (subjects 19, 20, 24, 33, and 36) and (C) nonresponders (subjects 21, 22, 23, 34, and 35). Diagonal lines delineate 4-fold change of the difference between posttreatment and pretreatment intensities above and below the  $x = y$  axis. (D) Box plots of upmodulated (upper panel) and downmodulated (lower panel) Abs with 4-fold change for nonresponders and responders. The box bounds the middle 50% of the values, and the median is denoted by the thick line. The whisker lines span 1.5 times the interquartile range. Data points beyond are considered as outliers and are shown as circles. Two-sided Wilcoxon rank sum test  $p$  value for the difference in the number of upmodulated Abs between nonresponders and responders is 0.0043 and in the number of downmodulated Abs is 0.429. \* $p < 0.05$ .



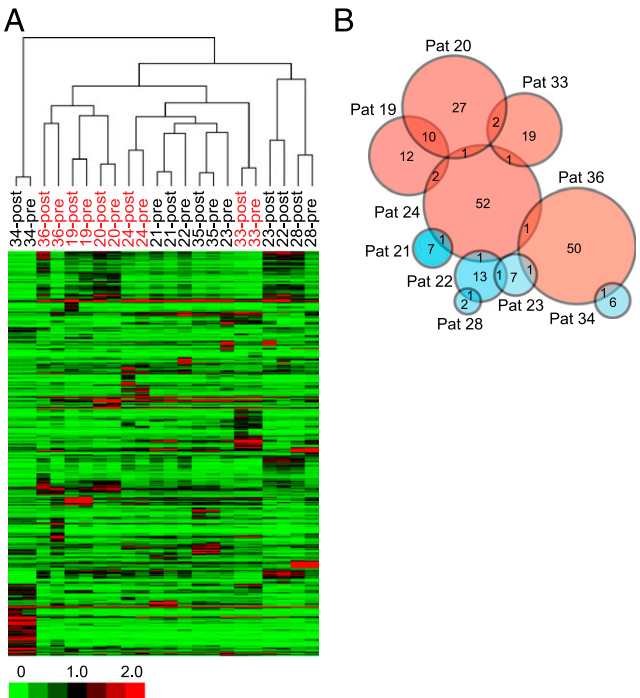


**FIGURE 2.** Profiling of Ab responses in cancer patients to CTLA-4 blockade and GM-CSF with protein microarrays. **(A)** Unsupervised clustering of median-centered, log<sub>2</sub>-transformed and normalized fluorescence intensities in pretreatment and posttreatment sera of 11 evaluable patients binding to proteins spotted on the arrays. Responders are highlighted in red and nonresponders in black. **(B)** Venn diagram showing the number of upmodulated Abs that are shared (shown by number in overlaps) or are unique in the 11 patients. Responders are represented by pink circles and nonresponders in blue. Sizes of circles approximate the number of Abs.

gether whereas responders 24 and 33 do not. The majority of the immune responses (both up- and downmodulated Abs) are unique for each patient, but there are also Abs shared across some patients

(Fig. 2B). Of the upmodulated Abs with pre- versus post-differences greater than 4-fold, 18.5% of the Abs induced in patients 19 and 20 are shared. The overlap between other responders is considerably less. The overlap between the responders versus the nonresponders is minimal. The list of shared Abs to which Abs are upmodulated by 4-fold is shown in Table 1. Notably, most of these Abs with Ab responses represent cell cycle-related or nuclear Abs, and ~30% of the Abs identified are kinases. Of the downmodulated Abs, the Abs detected are largely unique between patients with very few shared Abs.

*Abs distribution induced by anti-CTLA-4 and GM-CSF*

To examine whether the Ab responses enhanced by treatment are derived from preexisting immune responses or from de novo responses, the raw fluorescence intensity values of both pretreatment sera and posttreatment sera were first plotted in order of increasing intensities for each array (Supplemental Fig. 1A, 1B). Normal mixture modeling with EM as implemented in the mclust package in R (14) was applied to the raw intensities for each pretreatment and posttreatment array to identify the boundary between Abs to which Abs are present at baseline (i.e., preexisting) and Abs to which Abs are not present at baseline (i.e., non-preexisting). Abs that were upmodulated by 2-fold in the post-treatment serum with respect to the pretreatment serum were distributed either to the non-preexisting group or the preexisting group (Fig. 3A, left panel). Odds ratios were then calculated to assess for the association between upmodulated Ab responses and preexisting Ab status compared with non-preexisting (Fig. 3A, right panel). A positive odds ratio denotes a higher probability of developing Abs to an Ag with a pretreatment preexisting Ab response. Two-sided Fisher exact tests were performed for each patient, and *p* values were adjusted for multiple comparisons with the Bonferroni method. All the clinical responders and four of six of the nonresponders have significant upmodulation of Abs that were preexisting compared with not, indicating that the upmodulated Abs by CTLA-4 blockade are more likely to be preexisting. Moreover, the clinical responders have a higher median

Table 1. List of shared Abs upmodulated by 4-fold with anti-CTLA-4 and GM-CSF treatment

Patients	Number of Shared Abs	Entrez Gene ID	Gene Symbol	Description
19 and 20	10	558	AXL	AXL receptor tyrosine kinase
		4916	NTRK3	Neurotrophic tyrosine kinase, receptor, type 3
		695	BTK	Bruton agammaglobulinemia tyrosine kinase
		53944	CSNK1G1	Casein kinase 1, $\gamma$ 1
		4350	MPG	N-methylpurine-DNA glycosylase
		1454	CSNK1E	Casein kinase 1, $\epsilon$
		904	CCNT1	Cyclin T1
		56924	PAK6	p21 protein (Cdc42/Rac)-activated kinase 6
		1455	CSNK1G2	Casein kinase 1, $\gamma$ 2
		3815	KIT	v-kit Hardy-Zuckerman 4 feline sarcoma viral oncogene homolog
19 and 24	2	199	AIF1	Allograft inflammatory factor 1
		1745	DLX1	Distal-less homeobox 1
20 and 33	2	4145	MATK	Megakaryocyte-associated tyrosine kinase
		5347	PLK1	Polo-like kinase 1
20 and 24	1	1453	CSNK1D	Casein kinase 1, $\delta$
24 and 33	1	121355	GTSF1	Gametocyte specific factor 1
24 and 36	1	51155	HN1	Hematological and neurologic expressed 1
24 and 21	1	29995	LMCD1	LIM and cysteine-rich domains 1
24 and 22	1	90011	KIR3DX1	Killer cell Ig-like receptor, three domains, X1
36 and 23	1	81442	OR6N2	Olfactory receptor, family 6, subfamily N, member 2
36 and 34	1	116496	FAM129A	Family with sequence similarity 129, member A
22 and 23	1	2556	GABRA3	$\gamma$ -Aminobutyric acid A receptor, $\alpha$ 3
22 and 28	1	389125	MUSTN1	Musculoskeletal, embryonic nuclear protein 1

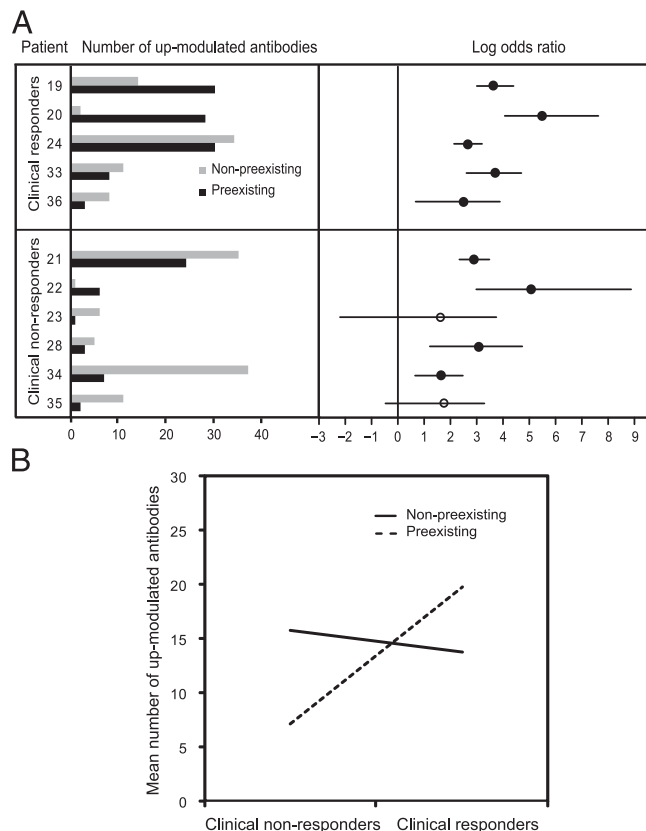


**FIGURE 3.** Association between upmodulated Abs with preexisting or non-preexisting Ab responses. Normal mixture modeling with EM was used to define the boundary for determining the presence or absence of preexisting Abs. **(A)** The left panel shows the number of 2-fold upmodulated Abs in the posttreatment serum to Ags where there are no preexisting Abs (light gray) and to Ags where there are preexisting Abs (dark gray) in the pretreatment serum for each patient. The right panel shows log odds ratios comparing 2-fold upmodulation for preexisting versus non-preexisting Ab groups for each patient. Significant log odds ratio values are shown as solid circles (significance determined as Bonferroni adjusted  $p$  value  $<0.05$  from performing two-sided Fisher exact test for each patient). **(B)** Interaction plot using multiplicative Poisson regression model with the number of Abs upmodulated, clinical response status, and pretreatment preexisting or not status as dependent variables. Response main effect  $p$  value:  $2.6 \times 10^{-8}$ ; pretreatment preexisting main effect  $p$  value:  $1.6 \times 10^{-5}$ ; and interaction  $p$  value:  $1.8 \times 10^{-6}$ .

odds ratio (39.6) compared with the clinical nonresponders (12.2), indicating that clinical responders were more likely to have upmodulated Ab responses to Ags that were preexisting.

To determine if there is any interaction between clinical response and enhancement of Ab response to Ags that were preexisting, a multiplicative Poisson regression model was fitted with the number of Abs upmodulated, clinical response status, and pretreatment preexisting or not status as dependent variables. With this analysis, there is a significant interactive effect between clinical response and preexisting Abs ( $p$  values: response main effect,  $2.6 \times 10^{-8}$ ; preexisting main effect,  $1.6 \times 10^{-5}$ ; interaction,  $1.8 \times 10^{-6}$ ) (Fig. 3B). The interaction plot shows that the responders have a higher number of Abs that were preexisting compared with the nonresponders, and the number of upmodulated Abs that were non-preexisting was similar for both responders and non-responders. For 4-fold increase in upmodulated Abs, the interaction showed the same trend as 2-fold upmodulation of Abs (Supplemental Fig. 1D, 1E).

### Induced immune responses to an Ag associated with clinical response

To examine whether any of the shared Ags could be relevant for tumor recognition, we focused on patients 19 and 20, who were clinical responders and shared the highest number of Ags. To prioritize the candidates for further study, upmodulated Ab responses were further sorted based on their posttreatment intensities to look for common candidates that have the highest signal intensities. One of these shared Ags is PAK6, a 75-kDa protein with a predicted N-terminal Cdc42/Rac interactive binding domain and a C-terminal kinase domain (18). Increases in Ab intensities to PAK6 were observed, whereas Ab intensities to the control Ag Influenza A H3N2 were not modulated with treatment (Fig. 4A). Detection of induced Abs to PAK6 protein could also be detected by ELISA (Supplemental Fig. 1F).

Ag-specific CD4<sup>+</sup> T cell responses to PAK6 were assessed ex vivo from cryopreserved PBMCs. As shown in Fig. 4B, patients 19 and 20 (both clinical responders) have increased percentage of IFN- $\gamma$ -producing CD4<sup>+</sup> T cells posttreatment when cocultured with PAK6, but not with another baculoviral purified protein, calcium/calmodulin-dependent protein kinase (CAMK). IL-17 or IL-4 production in response to these Ags was not detected. No T cell response is observed with PBMCs from patient 23 (a clinical nonresponder) to PAK6. These results show that Ag-specific T cell responses to Ags identified by our Ab screen can also be enhanced after treatment with CTLA-4 blockade.

Western blotting and immunohistochemical staining was performed to assess PAK6 expression in prostate cancers. Compared to two immortalized, non-tumorigenic, human prostate epithelial cell lines, PWR-1E (19) and RWPE (20), which expressed PAK6, we observed that PAK6 expression was higher in several prostate cancer cell lines, such as PC3 and CWR22, was similar for DU145, and was lower in LNCAP (Fig. 5A). Expression of PAK6 is thus variable in prostate cancer cell lines suggesting aberrant regulation of the protein in cancer cells. Expression of PAK6 was also observed in immunohistochemical staining of 16 primary human prostate tumors as has been previously observed for prostate tumors, and the prostate tumor biopsy from patient 20 similarly demonstrated a high level of expression of PAK6 (Fig. 5B). Prostate biopsies were not available from patient 19.

### Immunization with PAK6 protects mice to tumor challenge

To determine whether PAK6 can be immunogenic in vivo, we immunized mice with recombinant human PAK6 mixed with CFA. Immunization with a xenogeneic homolog may enhance immunogenicity to self-antigens (21). Human PAK6 shares 92% protein homology with mouse Pak6. Although spontaneous immune responses to PAK6 were not detected, immunization with recombinant purified human PAK6 protein led to the generation of PAK6-specific Abs (Fig. 6A) and proliferative T cell responses to human PAK6 protein (Fig. 6B). IFN- $\gamma$  T cell responses to both human and mouse Pak6 proteins were also observed with splenocytes from mice immunized with human PAK6 (Supplemental Fig. 2). Mice did not develop any apparent toxicity with this immunization, including signs of autoimmunity.

To assess whether inducing an immune response to PAK6 can lead to anti-tumor activity, we again immunized mice with either PBS or PAK6 protein and then challenged these mice with syngeneic prostate cancer cell lines. Fourteen days after the second immunization, treated C57BL/6 mice were challenged with  $2 \times 10^5$  Tramp mouse prostate cancer cells (22), and treated FVB mice were injected with  $2 \times 10^5$  Myc-Cap mouse prostate cancer cells (23). Both cell lines expressed endogenous mouse Pak6. Immu-

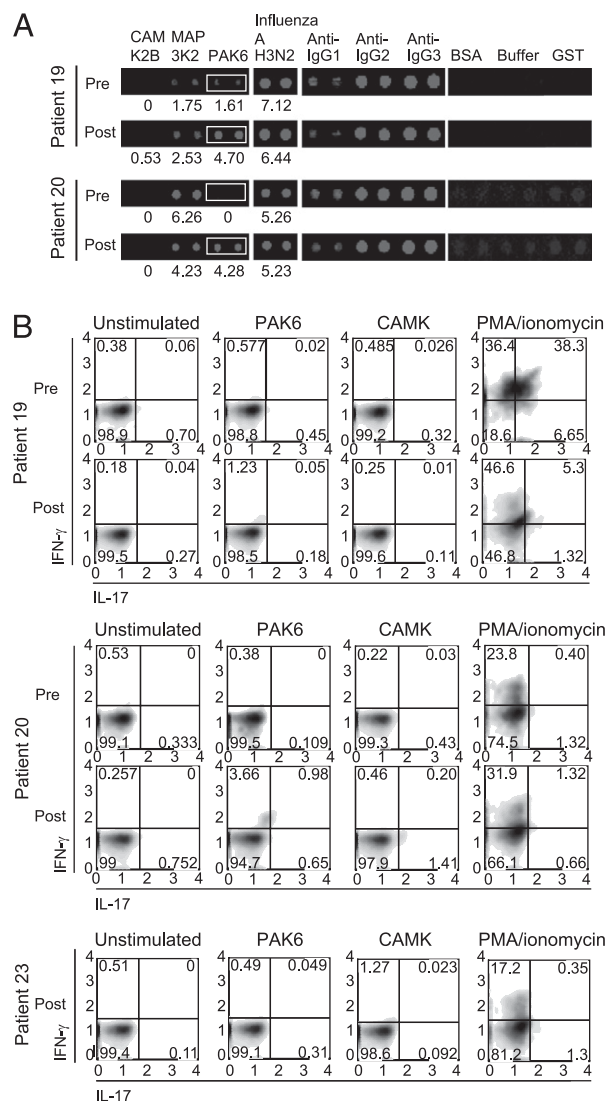


**FIGURE 4.** Detection of Ab and T cell responses to the candidate Ag PAK6. **(A)** Images of protein arrays showing levels of human IgG binding to PAK6 protein in the pretreatment and posttreatment sera of clinical responders (patients 19 and 20). Control proteins and Abs are also shown. Numbers shown below the PAK6 and influenza A Ag are the median-centered, log<sub>2</sub>-transformed and normalized fluorescence values. **(B)** Flow cytometry of pretreatment and posttreatment PBMCs from clinical responders (patients 19 and 20) and flow cytometry of posttreatment PBMCs from a clinical nonresponder (patient 23) that had been incubated with media alone, PAK6 protein, CAMK protein, or PMA plus ionomycin for 48 h and then stained for CD4 and intracellular IFN-γ and IL-17. CD4<sup>+</sup> T cells were gated upon and analyzed for cytokine production. Axes are log<sub>10</sub> fluorescence of IFN-γ (y-axis) and IL-17 (x-axis) staining. The number in each quadrant indicates the percentage of cells in that quadrant.

nization with PAK6 induces anti-tumor responses in both the Tramp and Myc-Cap models of prostate cancer (Fig. 6C). These results indicate that immunity to Pak6 can contribute to anti-tumor effects in vivo against prostate cancer cells expressing endogenous mouse Pak6.

## Discussion

CTLA-4 blockade is currently being evaluated clinically in many different solid and hematologic malignancies. Treatment with anti-CTLA-4 Abs presumably potentiates immunosurveillance to endogenous tumor Ags by relieving a crucial immune checkpoint. However, the specific endogenous Ag response has been difficult

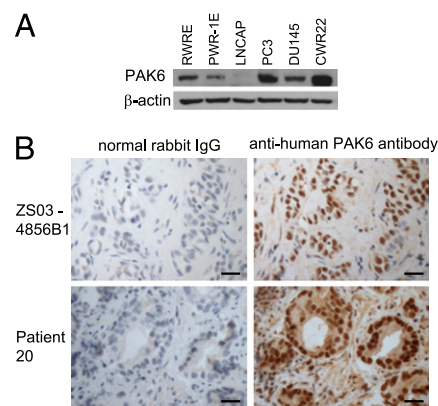


**FIGURE 5.** Expression and localization of PAK6 in prostate cancer. **(A)** Western blots of prostate cancer cell lines (LNCAP, PC3, DU145, and CWR22) and human prostate epithelial cell lines (PWR-1E and RWPE) carried out with anti-PAK6 and anti-β-actin Ab. **(B)** Immunohistochemistry of prostate tumor biopsy of responder patient 20 and a representative prostate tumor with anti-PAK6 Abs and with control rabbit IgG. Scale bar, 50 μm.

to define, particularly in the absence of a coadministered vaccine where the vaccine Ags may be known. Nevertheless CTLA-4 blockade can induce clinical responses in the absence of a vaccine. None of our patients received an administered tumor vaccine as part of their treatment, so their clinical effects must be de-

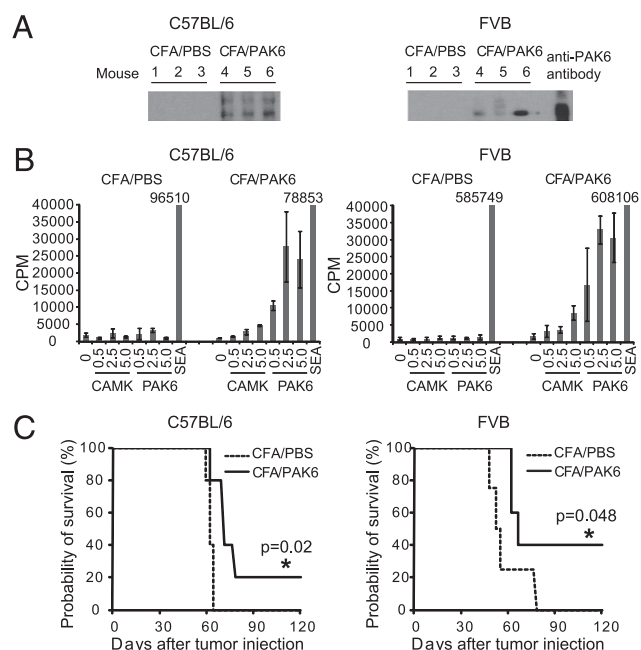


**FIGURE 6.** Immunogenicity and anti-tumor activity of PAK6 immunization. **(A)** Western blots carried out with sera from C57BL/6 and FVB mice immunized twice with PBS plus CFA or with human PAK6 plus CFA (three mice/group). **(B)** Proliferation assays carried out with inguinal lymph node cells pooled from immunized C57BL/6 and FVB mice incubated with media alone or with the protein as shown. Concentrations are in micrograms per milliliter. Proliferation was measured as radioactive counts per minute of [<sup>3</sup>H]thymidine incorporation. Error bars denote ±SDs of triplicate wells. **(C)** Kaplan-Meier survival curve of tumor challenge for C57BL/6 and FVB mice immunized twice with PBS plus CFA or human PAK6 plus CFA (five mice/group) and challenged 14 d later with Tramp cells. Tumors were measured three times a week, and mice were sacrificed when the tumor size reached 2 cm per institutional guidelines. The *p* values were calculated by using the log-rank test (SPSS; IBM). \**p* ≤ 0.05.

pendent on endogenous Ags. By using protein microarrays representing approximately one-third of the human proteome, we were able to profile the Ab responses induced with treatment to a broad spectrum of autoantigens. Moreover, a significant proportion of patients clinically responded to our treatment allowing us to examine whether Ag-specific responses could distinguish the clinical responders from nonresponders.

Based on these Ab responses, clinical responders developed a broader immune response as seen by the induced Abs to a greater number of endogenous Ags compared with the nonresponders. This difference was observed at 4-fold but not at 2-fold upmodulation of Abs indicating that the induced responses were also at higher intensities for the responders compared with the nonresponders. The modulated Ab responses were quite diverse, and there was very little overlap between the Ags identified in responders versus the nonresponders. These results show that patients who can clinically respond to treatment may also be immunologically distinct from nonresponders based on their autoantibody profiles. These differences could reflect the capacity of tumors in different patients to avoid immunosurveillance. Alternatively, the clinical responders may have tumors that are inherently more immunogenic or may have differing levels of tumor-associated immunosuppression. The majority of the Ags are unique for each patient, which could also reflect the diversity of their T and B cell repertoires and/or the heterogeneity of Ags expressed in prostate tumors. Although common pathways could be affected in cancer, different genetic alterations are observed in cancer patients (24, 25), which can give rise to an individualized antigenic milieu. Therefore, by modulating the immune system to recognize patient-specific endogenous Ags, CTLA-4 blockade could represent a form of personalized immunotherapy.

Another unresolved question regarding the treatment's mechanism of action is whether CTLA-4 blockade enhances preexisting immune responses or whether the treatment potentiates *de novo* Ag-specific responses. In all of our patients, we did not see any modulation of Ab responses to the control Ag Influenza A H3N2, supporting the notion that the treatment-induced modulation of Abs reflects the Ag milieu in the host. Ab responses were in fact induced to Ags both with and without detectable preexisting Abs prior to treatment. This is exemplified with PAK6, to which patient 19 had low levels of Ab prior to treatment, whereas patient 20 had undetectable levels prior to treatment. Notably, clinical responders were more likely than nonresponders to generate Abs against Ags to which preexisting Abs could be detected. These results suggest that induction of preexisting rather than *de novo* (non-preexisting) immune responses may be important in generating anti-tumor activity in CTLA-4 blockade therapy. With one of the clinical responders (patient 19), detectable preexisting IgG to PAK6 could be detected, but no T cell response to PAK6 could be detected at baseline. After treatment, a CD4 T cell response to PAK6 was induced coinciding with an enhancement of IgG responses. These results would indicate that an immune response to PAK6 was generated spontaneously in the patient but was subsequently dampened perhaps by tumor-induced immunosuppression. Nevertheless, relieving a crucial immunologic checkpoint with CTLA-4 blockade may be sufficient to recover immune responses to such tumor-associated Ags.

Abs that were downmodulated were also detected in CTLA-4 blockade therapy. However, the number of downmodulated Abs between the responders and nonresponders were not significantly different. Total levels of IgG were not significantly changed with treatment, so these changes could not be due to dilution. However, the mechanism for downmodulation of Abs by CTLA-4 blockade is unclear at present.

Most of the Ags with induced autoantibodies after treatment were intracellular proteins. Presumably, immune responses could have been initiated to these Ags as they are released from dying cells, especially as tumor cells have a propensity for increased cell turnover as well as for apoptosis and necrosis (26). All of our patients received and clinically progressed on androgen deprivation therapy, which would have also induced cancer cell death and release of Ags. However, there may be insufficient danger signals to drive an effective immune response in the absence of CTLA-4 blockade. The Ag that we focused upon, PAK6, could be considered a novel tumor-associated Ag. PAK6 is expressed in prostate cancer and is known to cotranslocate into the nucleus with androgen receptor in response to androgen and inhibits the transcriptional activity of androgen receptor (18). Alterations in PAK6 itself or in the regulation and expression of PAK6 could render PAK6 more immunogenic. Indeed, missense mutations have already been detected in PAK6 in the prostate cancer cell lines PC3 and LAPC9 as well as in primary prostate cancer (MSKCC Prostate Oncogenome Project; <http://cbio.mskcc.org/prostate-portal/>). PAK6 has to be recognized by T cells to mediate anti-tumor effects. As we have demonstrated, Pak6-specific T cell responses are induced in the immunized mice, and PAK6-specific T cell responses could be detected directly in the posttreatment blood of the clinical responders who have induced Ab responses to this Ag. The reactive T cells of the patients produced IFN- $\gamma$  to PAK6 that was consistent with a Th1 response and were of a magnitude beyond what has been spontaneously detected with previously described prostate-associated Ags (27).

Whether these autoantigens represent immune targets that can mediate anti-tumor immunity or represent bystander Ags resulting from tumor cell death in humans remains a critical question. Nevertheless, we found that PAK6 immunization can lead to tumor protection in both the Myc-Cap and Tramp transplantable models of prostate cancer, indicating that inducing immunity to such a self-protein can in fact lead to anti-tumor responses. However, the protection afforded by PAK6 immunization was not complete, suggesting that immune recognition of other Ags can also contribute to anti-tumor responses. Knockdown of Pak6 with small interfering RNA has been shown to inhibit prostate cancer growth in nude mice (28) and increase radiosensitivity of prostate cancer cell lines (29), further supporting PAK6 as a viable target for cancer therapy.

Although our patient cohort is relatively small, the number of clinical responses we observed provided a unique opportunity to characterize how the breadth of the Ag immune response induced by treatment is associated with clinical outcome. Our results with PAK6 represent only one of the Ags that we have identified with our approach. Nevertheless, immune responses to more than one cancer Ag will likely be required for maximal efficacy. As more treated patients are analyzed with this Ab profiling, other novel Ags will undoubtedly be identified including additional shared targets. Moreover, this approach may provide us with an immunologic perspective into not only molecular aberrations in these tumors but also the heterogeneity of these alterations between patients. Alternatively, patients who developed treatment-induced immune-related adverse events may also provide unique opportunities perhaps to identify relevant autoantigens that might mediate these side effects. We did not see specific toxicities (e.g., only three patients had diarrhea) at sufficient frequency to assess for these associations. Nevertheless, defining an immune profile that is associated with specific side effects could also allow for improved patient selection for these immune therapies, especially as ipilimumab is more widely used. Finally, understanding the nature and targets of the adaptive immune response elicited by immune



checkpoint blockade could result in the development of improved multitargeted vaccines, which could direct the immune response more specifically to the tumor, thus increasing the therapeutic efficacy and perhaps reducing the frequency of immune-mediated side effects seen with immunotherapy.

## Acknowledgments

We acknowledge the University of California, San Francisco (UCSF) Tissue Core for sectioning, Loretta Chan of the UCSF Mt. Zion Immunohistochemistry Core Laboratory for immunohistochemistry staining, Vivian Huey from the UCSF Department of Hematology/Oncology for obtaining patients' tissue samples, and Vivian Weinberg from the UCSF Biostatistics and Computational Biology Core Facility for assistance.

## Disclosures

The authors have no financial conflicts of interest.

## References

- Greenwald, R. J., G. J. Freeman, and A. H. Sharpe. 2005. The B7 family revisited. *Annu. Rev. Immunol.* 23: 515–548.
- Brücher, J., I. Domke, C. H. Schröder, and H. Kirchner. 1984. Experimental infection of inbred mice with herpes simplex virus. VI. Effect of interferon on in vitro virus replication in macrophages. *Arch. Virol.* 82: 83–93.
- Leach, D. R., M. F. Krummel, and J. P. Allison. 1996. Enhancement of antitumor immunity by CTLA-4 blockade. *Science* 271: 1734–1736.
- Link, K. A., S. Balasubramaniam, A. Sharma, C. E. Comstock, S. Godoy-Tundidor, N. Powers, K. H. Cao, A. Haelens, F. Claessens, M. P. Revelo, and K. E. Knudsen. 2008. Targeting the BAF57 SWI/SNF subunit in prostate cancer: a novel platform to control androgen receptor activity. *Cancer Res.* 68: 4551–4558.
- Hernández, J., A. Ko, and L. A. Sherman. 2001. CTLA-4 blockade enhances the CTL responses to the p53 self-tumor antigen. *J. Immunol.* 166: 3908–3914.
- Fassò, M., R. Waitz, Y. Hou, T. Rim, N. M. Greenberg, N. Shastri, L. Fong, and J. P. Allison. 2008. SPAS-1 (stimulator of prostatic adenocarcinoma-specific T cells)/SH3GLB2: a prostate tumor antigen identified by CTLA-4 blockade. *Proc. Natl. Acad. Sci. USA* 105: 3509–3514.
- Yuan, J., S. Gnjatic, H. Li, S. Powel, H. F. Gallardo, E. Ritter, G. Y. Ku, A. A. Jungbluth, N. H. Segal, T. S. Rasalan, et al. 2008. CTLA-4 blockade enhances polyfunctional NY-ESO-1 specific T cell responses in metastatic melanoma patients with clinical benefit. *Proc. Natl. Acad. Sci. USA* 105: 20410–20415.
- Fong, L., S. S. Kwek, S. O'Brien, B. Kavanagh, D. G. McNeel, V. Weinberg, A. M. Lin, J. Rosenberg, C. J. Ryan, B. I. Rini, and E. J. Small. 2009. Potentiating endogenous antitumor immunity to prostate cancer through combination immunotherapy with CTLA4 blockade and GM-CSF. *Cancer Res.* 69: 609–615.
- Jinushi, M., F. S. Hodi, and G. Dranoff. 2006. Therapy-induced antibodies to MHC class I chain-related protein A antagonize immune suppression and stimulate antitumor cytotoxicity. *Proc. Natl. Acad. Sci. USA* 103: 9190–9195.
- Armitage, J. O. 1998. Emerging applications of recombinant human granulocyte-macrophage colony-stimulating factor. *Blood* 92: 4491–4508.
- Markowicz, S., and E. G. Engleman. 1990. Granulocyte-macrophage colony-stimulating factor promotes differentiation and survival of human peripheral blood dendritic cells in vitro. *J. Clin. Invest.* 85: 955–961.
- Hurwitz, A. A., T. F. Yu, D. R. Leach, and J. P. Allison. 1998. CTLA-4 blockade synergizes with tumor-derived granulocyte-macrophage colony-stimulating factor for treatment of an experimental mammary carcinoma. *Proc. Natl. Acad. Sci. USA* 95: 10067–10071.
- Eisen, M. B., P. T. Spellman, P. O. Brown, and D. Botstein. 1998. Cluster analysis and display of genome-wide expression patterns. *Proc. Natl. Acad. Sci. USA* 95: 14863–14868.
- Team, R. D. C. 2005. *R: A Language and Environment for Statistical Computing*. R Foundation for Statistical Computing, Vienna, Austria.
- Gentleman, R. C., V. J. Carey, D. M. Bates, B. Bolstad, M. Dettling, S. Dudoit, B. Ellis, L. Gautier, Y. Ge, J. Gentry, et al. 2004. Bioconductor: open software development for computational biology and bioinformatics. *Genome Biol.* 5: R80.
- Biragyn, A., P. A. Ruffini, C. A. Leifer, E. Klyushnenkova, A. Shakhov, O. Chertov, A. K. Shirakawa, J. M. Farber, D. M. Segal, J. J. Oppenheim, and L. W. Kwak. 2002. Toll-like receptor 4-dependent activation of dendritic cells by beta-defensin 2. *Science* 298: 1025–1029.
- Hudson, M. E., I. Pozdnyakova, K. Haines, G. Mor, and M. Snyder. 2007. Identification of differentially expressed proteins in ovarian cancer using high-density protein microarrays. *Proc. Natl. Acad. Sci. USA* 104: 17494–17499.
- Yang, F., X. Li, M. Sharma, M. Zarnegar, B. Lim, and Z. Sun. 2001. Androgen receptor specifically interacts with a novel p21-activated kinase, PAK6. *J. Biol. Chem.* 276: 15345–15353.
- Webber, M. M., D. Bello, H. K. Kleinman, D. D. Wartinger, D. E. Williams, and J. S. Rhim. 1996. Prostate specific antigen and androgen receptor induction and characterization of an immortalized adult human prostatic epithelial cell line. *Carcinogenesis* 17: 1641–1646.
- Webber, M. M., D. Bello, H. K. Kleinman, and M. P. Hoffman. 1997. Acinar differentiation by non-malignant immortalized human prostatic epithelial cells and its loss by malignant cells. *Carcinogenesis* 18: 1225–1231.
- Fong, L., C. L. Ruegg, D. Brockstedt, E. G. Engleman, and R. Laus. 1997. Induction of tissue-specific autoimmune prostatitis with prostatic acid phosphatase immunization: implications for immunotherapy of prostate cancer. *J. Immunol.* 159: 3113–3117.
- Foster, B. A., J. R. Gingrich, E. D. Kwon, C. Madias, and N. M. Greenberg. 1997. Characterization of prostatic epithelial cell lines derived from transgenic adenocarcinoma of the mouse prostate (TRAMP) model. *Cancer Res.* 57: 3325–3330.
- Watson, P. A., K. Ellwood-Yen, J. C. King, J. Wongvipat, M. M. Lebeau, and C. L. Sawyers. 2005. Context-dependent hormone-refractory progression revealed through characterization of a novel murine prostate cancer cell line. *Cancer Res.* 65: 11565–11571.
- Jones, S., X. Zhang, D. W. Parsons, J. C. Lin, R. J. Leary, P. Angenendt, P. Mankoo, H. Carter, H. Kamiyama, A. Jimeno, et al. 2008. Core signaling pathways in human pancreatic cancers revealed by global genomic analyses. *Science* 321: 1801–1806.
- Taylor, B. S., N. Schultz, H. Hieronymus, A. Gopalan, Y. Xiao, B. S. Carver, V. K. Arora, P. Kaushik, E. Cerami, B. Reva, et al. 2010. Integrative genomic profiling of human prostate cancer. *Cancer Cell* 18: 11–22.
- Tesniere, A., T. Panaretakis, O. Kepp, L. Apetoh, F. Ghiringhelli, L. Zitvogel, and G. Kroemer. 2008. Molecular characteristics of immunogenic cancer cell death. *Cell Death Differ.* 15: 3–12.
- McNeel, D. G., L. D. Nguyen, W. J. Ellis, C. S. Higano, P. H. Lange, and M. L. Disis. 2001. Naturally occurring prostate cancer antigen-specific T cell responses of a Th1 phenotype can be detected in patients with prostate cancer. *Prostate* 47: 222–229.
- Wen, X., X. Li, B. Liao, Y. Liu, J. Wu, X. Yuan, B. Ouyang, Q. Sun, and X. Gao. 2009. Knockdown of p21-activated kinase 6 inhibits prostate cancer growth and enhances chemosensitivity to docetaxel. *Urology* 73: 1407–1411.
- Zhang, M., M. Siedow, G. Saia, and A. Chakravarti. 2010. Inhibition of p21-activated kinase 6 (PAK6) increases radiosensitivity of prostate cancer cells. *Prostate* 70: 807–816.